

Quadrupole effects in NMR spectra of spatially modulated structures

I. P. Aleksandrova, Yu. N. Moskvich, S. Grande, and A. I. Kriger

Physics Institute, Siberian Division, USSR Academy of Sciences

(Submitted 18 January 1983; resubmitted 14 April 1983)

Zh. Eksp. Teor. Fiz. **85**, 1335–1348 (October 1983)

A model is proposed for a quantitative description of the dependence of the anomalous shape of the NMR line in modulated structures on the crystal orientation in a magnetic field, and a method is proposed for determining the electric field gradient (EFG) near the maximum amplitudes of the displacement waves. It is proposed to describe the EFG distribution in terms of position color symmetry. It is observed that resonance experiments demonstrate the conservation of the generalized symmetry in the commensurate–incommensurate phase transition.

PACS numbers: 76.60. – k, 76.20. + q

I. INTRODUCTION

The first radiospectroscopy investigations of spatially modulated structures revealed a number of anomalous phenomena in the NQR^{1,2} and NMR^{3,4} spectra.

The anomalous line shape of the resonance spectrum and the temperature dependence of the frequencies of the spectral distribution peaks were explained from the viewpoint of modulation of the electric field gradient (EFG), at the location of the nucleus, by an incommensurate displacement wave.^{1–4} A quantitative description, assuming modulation of the EFG by a single Fourier harmonic of the displacement field (modulation by a plane wave)^{4–6} and in the phase-soliton approximation^{7–9} has yielded very important information on the structure of incommensurate phases of a number of ferroelectrics. For example, NQR spectra, and later NMR and EPR spectra, provided direct experimental confirmation of the existence of a lattice of phase solitons near the “lock-in” transition (T_c). With rise in temperature, this state was observed to turn into purely sinusoidal modulation near the high-temperature transition T_I .^{1,2,7–11}

Even the first NMR experiments have shown that the shape of the anomalous line depends on the crystal orientation in the magnetic field. It was shown in Ref. 12 that the orientation in the magnetic field. It was shown in Ref. 12 that the orientation dependences of the peaks of the anomalous spectral distribution can be used to determine the EFG tensor near the maximum amplitudes of the displacement wave. Regular investigations of the EFG in different temperature regions of the incommensurate phase can yield considerably more complete information on its structure than the temperature dependence. Of greater interest, however, is apparently the possibility of investigating the symmetry properties of the incommensurate structure.

The method of determining the EFG in a three-dimensionally periodic lattice¹³ cannot be applied directly to an incommensurably modulated structure. Just as in the description of the temperature dependence of the anomalous line shape, it is necessary here to develop a new quantitative description. The EFG tensor at the ⁸⁷Rb nucleus in Rb₂ZnCl₄ was determined in Ref. 12 in the immediate vicinity of the high-temperature phase-transition point T_I , where the incommensurate displacements are very small and the modulation effect can be easily deduced from the experimen-

tal curves and from certain general considerations.

We formulate in this paper the selection rules for the nonzero components of the modulation-correction tensor. This permits, in each concrete case, to write down the general form of the EFG tensor for the incommensurate phase and interpret the experimentally observed orientation dependences of the line shape at any temperature, except in the vicinity of the lock-in transition. The quantitative model is compared with the experimental data, the spectra are interpreted, and the EFG tensor of ⁸⁷Rb in the incommensurate phases of Rb₂ZnCl₄ and Rb₂ZnBr₄ is determined at several temperatures.

It is known that incommensurate modulation of lattice displacements leads to loss of three-dimensional periodicity of the crystal.^{14,15} We show in this paper that in resonance experiments the generalized symmetry is conserved in the phase transition from the initial to the incommensurably modulated phase. It is proposed to describe the local properties of the incommensurate phase (the EFG at the point of localization of the nucleus) in term of positional color symmetry.

II. THE MODEL

The EFG tensor component in the lattice position $\{S\}$ below the phase transition point can be represented by a series in powers of the displacements in the “frozen” soft mode¹⁶:

$$V_{ij}^j\{S\} = V_{ij}^0\{S\} + \sum_1^N A_k U_k + \sum_1^N B_{kk'} U_k U_{k'} + \dots \quad (1)$$

The expansion is carried out near the equilibrium positions of the initial phase,

$$A_k = \frac{\partial V_{ij}\{S\}}{\partial x_k}, \quad B_{kk'} = \frac{\partial^2 V_{ij}}{\partial x_k \partial x_{k'}},$$

the displacements are observed along the x direction, and the summation is over all the N nuclei that contribute to the EFG at the nucleus S .

Approximating the displacement field in the incommensurate phase by a single Fourier harmonic, we write in accord with Ref. 17

$$U^j = U_0 \cos \varphi = U_0 \cos(q_0 z_i + \Phi_0); \quad (2)$$

here

$$\Phi_0 = \text{const}, \quad q_0 = (1 - \delta) q_s, \quad \delta \ll 1, \quad q_s = \tau/p,$$

τ is the reciprocal-lattice vector, p is an integer, and z_l numbers the lattice positions that are translationally equivalent in the initial phase along the modulation direction z .

Using (2), we can rewrite (1) in terms of the real phase and of the amplitude of the order-parameter:

$$V_{ij}^j \{S\} = V_{ij}^0 \{S\} + \sum_1^N A_k U_{0k} \cos(q_0 z_l + \Phi_0) + \sum_1^N B_{hk} U_{0k} U_{0k}' \cos^2(q_0 z_l + \Phi_0). \quad (3)$$

It can be seen from (3) that in the incommensurate phase the EFG varies quasi-continuously along the displacement profile, between maximum-amplitude values corresponding to $\cos \varphi_l = +1$ and -1 .

We assume next that the main changes of the EFG below T_l are due to incommensurate displacements of the nuclei under observation. Then

$$V_{ij}^j \{S\} = V_{ij}^0 \{S\} + A U_0 \cos \varphi_l + B U_0^2 \cos^2 \varphi_l + \dots \quad (4)$$

We note that this rather crude approximation holds well for a description of the temperature dependences of the shapes of resonance lines.^{5,7-9}

The EFG in the incommensurate phase can thus be represented as a sum of the EFG tensor in the lattice position $\{S\}$ of the initial structure (of the basic lattice) and the tensor $\Delta V_{ij} \{S\}$ of the modulation corrections:

$$V_{ij}^j = V_{ij}^0 \{S\} + \Delta V_{ij} \{S\}. \quad (5)$$

The representation in the form (5) is convenient for a transition to a description of the symmetry properties in terms of positional color symmetry, where $\Delta V_{ij} \{S\}$ plays the role of the color details with cosinusoidal distribution, and V_{ij}^0 represents the properties of the basic lattice.

Because of the irrational ratio of the period of the basic lattice to the period of the modulating wave, the displacement function is not periodic in the running coordinate z_l . From the viewpoint of classical symmetry, the three-dimensional spatial periodicity of such a crystal is disturbed. It is impossible to find points with like "color" on a finite segment of the displacement profile. If, however, $l \rightarrow \infty$, "quasi-single-color" points not connected by a constant translation can be observed. On each finite displacement-profile segment there is a loss of the symmetry plane \bar{m} of the initial structure. It is easy to show that one-dimensional modulation destroys also other elements of the Fedorov symmetry group of the initial three-dimensional cell.

If all the states encountered on a profile of infinite length are transferred to the cosinusoid segment corresponding to the period of the modulating wave, the lattice states fill continuously this segment, which can be called the "modulation cell."¹⁸ This operation recalls the referral of all the reciprocal-lattice vectors the first Brillouin zone. The modulation cell includes the entire possible set of lattice states of the given profile, the "color" in it varies continuously, and a translation appears, namely, points of like color are connected by the modulation period, and in each half of this period

are encountered states connected by the mirror-reflection plane and by a glide through half the period along z .

Let us consider the EFG at nuclei corresponding to the positive and negative maximum amplitudes of the displacements in the modulation cell. The EFG tensors of these lattice positions differ only in the signs of two off-diagonal components in accord with the mirror-reflection transformation. This imposes stringent restrictions on the form of the modulation-correction tensor, and determines the selection rule for its nonzero components: linear corrections $\Delta V_{ij} = \alpha_{ij} (\pm U_0)$ with alternating signs of U_0 can be introduced only for off-diagonal components and only if the corresponding components of the EFG tensor of the basic lattice are equal to zero. This takes place if the "working" nucleus in the initial structure is located in a particular position. Corrections to diagonal components are always quadratic in U_0 : $\Delta V_{ii} = \alpha_{ii} U_0^2$.

The relations between the frequency of the resonance line and the EFG at the nucleus are different for NQR, NMR, and EPR spectroscopy. In all cases, however, as a consequence of (4), the resonance frequency can be represented as a series in powers of the order parameter, with the coefficients determined from the EFG tensor components. In studies involving the description of the line shape in a modulated structure, these coefficients were empirical constants and were determined from the experimental temperature dependences of the frequencies of the spectral maxima.

In ordinary structures, the NMR spectrum consists of a relatively small number of singlet lines, each of which corresponds to one of the lattice positions of the working nucleus. In an incommensurate structure the infinite number of states filling the cosinusoid of the displacement profile contributes to the frequency spectrum, and the spectral density function is defined as³⁻⁵

$$f(\nu) = \text{const} / (d\nu/dz_l). \quad (6)$$

In the plane-wave-modulation approximation the line shape is a wide frequency continuum bounded by the maxima of the spectral density at the zeros of the function $d\nu/dz_l$. The terminal peaks correspond to the displacement-profile points with $\varphi_{1,2} = 0$ and π , i.e., to the positive and negative maximum amplitudes of the displacements. When (4) is approximated by only even powers of U_0 , one of the edge peaks corresponds as before to the maximum amplitude of the displacements, while the second peak corresponds to $\varphi_2 = \pi/2$, i.e., $U^j = 0$. A third singularity can appear in the spectrum if $A < 2B$.⁵⁻⁷

The frequency of the edge peaks at constant temperature depends on the crystal orientation in the magnetic field. To write down in explicit form the connection between the frequency and the EFT-tensor components it is necessary to specify the form of the tensor V_{ij}^j as applied to the investigated crystal. The working ⁸⁷Rb nuclei in the structure of the initial phases of Rb_2ZnCl_4 and Rb_2ZnBr_4 are located in a mirror-symmetry plane in two structurally nonequivalent positions (Rb1 and Rb2).^{12,19} Therefore in a fixed coordinate frame $a \parallel x, b \parallel y, c \parallel z$, where $a < c < b$ are the axes of the rhombohedral cell P_{mcn} , the EFG tensor has only one nonzero off-diagonal component V_{yz}^0 . In accord with the selection rules

formulated above, the tensor of the modulation corrections takes the form

$$\Delta V_{ij} = \begin{vmatrix} \alpha_{11}U_0^2 & \alpha_{12}(\pm U_0) & \alpha_{13}(\pm U_0) \\ & \alpha_{22}U_0^2 & 0 \\ & & \alpha_{33}U_0^2 \end{vmatrix}. \quad (7)$$

We have observed in our measurements only the central lines of the spectrum of ^{87}Rb (1,2) ($\pm \frac{1}{2} \rightarrow -\frac{1}{2}$ transition), whose positions are determined by the second-order quadrupole shift $\Delta\nu$ from the Larmor frequency ν_L . Introducing (5) and (7) in the known relations for the three mutually orthogonal rotations of a crystal¹³ and discarding all U_0 powers higher than the second, we obtain equations that describe the orientational dependences of the frequencies of the terminal peaks of the continua in the coordinate frame $a||x, b||y, c||z$.

For $a \perp H_0$ we have

$$\begin{aligned} \Delta\nu_x^j &= n_x + q_x \cos 2\theta_x + r_x \sin 2\theta_x + w_x \cos 4\theta_x + v_x \sin 4\theta_x, \\ n_x &= L[18c_2(V_{xx} + \alpha_{11}U_0^2)^2 + (c_2 - 4c_1)(V_{yy} - V_{zz} + \alpha_{22}U_0^2 - \alpha_{33}U_0^2)^2 \\ &\quad + 4(c_2 - 4c_1)V_{yz}^2 + 16(c_2 - c_1)(\alpha_{12}^2 - \alpha_{13}^2)U_0^2], \\ q_x &= L[12c_2(V_{xx} + \alpha_{11}U_0^2)(V_{yy} - V_{zz} + \alpha_{22}U_0^2 - \alpha_{33}U_0^2) + 16(c_2 + c_1)(\alpha_{13}^2 - \alpha_{12}^2)U_0^2], \\ r_x &= L[-24c_2(V_{xx} + \alpha_{11}U_0^2)V_{yz} + 32(c_2 + c_1)\alpha_{12}\alpha_{13}U_0^2], \\ w_x &= L(c_2 + 4c_1)[(V_{yy} - V_{zz} + \alpha_{22}U_0^2 - \alpha_{33}U_0^2)^2 - 4V_{yz}^2], \\ v_x &= -4L[(c_2 + 4c_1)(V_{yy} - V_{zz} + \alpha_{22}U_0^2 - \alpha_{33}U_0^2)V_{yz}], \\ c_1(m) &= 4[(J + 3/2)(J - 1/2) - 6(m - 1/2)^2], \\ c_2(m) &= 2[(J + 3/2)(J - 1/2) - 3(m - 1/2)^2], \end{aligned} \quad (8a)$$

$L = \frac{1}{4} \cdot \frac{1}{376} \nu_L$. For $b \perp H_0$ we have

$$\begin{aligned} \Delta\nu_y^j &= n_y + q_y \cos 2\theta_y + r_y \sin 2\theta_y + w_y \cos 4\theta_y + v_y \sin 4\theta_y, \\ n_y &= L[18c_2(V_{yy} + \alpha_{22}U_0^2)^2 + (c_2 - 4c_1)(V_{zz} - V_{xx} + \alpha_{33}U_0^2 - \alpha_{11}U_0^2)^2 + 4(c_2 - 4c_1)\alpha_{13}^2U_0^2 + 16(c_2 - c_1)(V_{yz}^2 + \alpha_{12}^2U_0^2)], \\ q_y &= L[12c_2(V_{yy} + \alpha_{22}U_0^2)(V_{zz} + \alpha_{33}U_0^2 - V_{xx} - \alpha_{11}U_0^2) - 16(c_2 + c_1)(V_{yz}^2 - \alpha_{12}^2U_0^2)], \\ r_y &= L[-24c_2(V_{yy} + \alpha_{22}U_0^2)\alpha_{13}U_0 + 32(c_2 + c_1)V_{yz}\alpha_{12}U_0], \\ w_y &= L(c_2 + 4c_1)[(V_{zz} - V_{xx} + \alpha_{33}U_0^2 - \alpha_{11}U_0^2)^2 - 4\alpha_{13}^2U_0^2], \\ v_y &= -4L[(c_2 + 4c_1)(V_{zz} - V_{xx} + \alpha_{33}U_0^2 - \alpha_{11}U_0^2)\alpha_{13}U_0]. \end{aligned} \quad (8b)$$

Analogous relations for $c \perp H_0$ are obtained by cyclic permutation of the indices xyz in (8a). Here θ is the angle between the direction of the magnetic field and the axis of a fixed system of coordinates in a plane perpendicular to the rotation axis.

The coefficients r and v in (8b) are positive for $+U_0$ and reverse sign for $-U_0$; the result are two frequencies $\Delta\nu_+$ and $\Delta\nu_-$ for each orientation, corresponding to the two terminal peaks. In periodic structures the signs of these coefficients are reversed if the structure contains nuclei that are related by Fedorov symmetry-group elements. When the rotation axis is parallel to the direction of the displacements in the modulation wave ($a \perp H_0$), the relation for $\Delta\nu_{\pm}^j$ contains only corrections quadratic in U_0 . At certain orientations of in rotations with $b \perp H_0$ and $c \perp H_0$ the coefficients of the corrections linear in U_0 are small and a third singularity that complicates the interpretation of the orientation dependences can appear in the spectrum. The orientation dependence of the frequency of this peak is defined for the time being on the basis of (6) and (7) as

$$\Delta\nu_{111}^j = \nu_0(\theta) + (\Delta r \sin 2\theta + \Delta v \sin 4\theta)^2/4(\Delta n + \Delta q \cos 2\theta + \Delta w \cos 4\theta), \quad (9)$$

where

$$\begin{aligned} \cos \varphi_3 &= (\Delta r \sin 2\theta + \Delta v \sin 4\theta)/2(\Delta n + \Delta q \cos 2\theta - \Delta w \cos 4\theta), \\ \Delta n, \Delta q, \Delta w &\sim U_0^2, \quad \Delta r, \Delta v \sim U_0. \end{aligned}$$

It can be seen from (9) that the phase φ_3 near which the third minimum of the function $d\nu/d\varphi$ is observed depends on the crystal orientation in the external field. The third singularity is not "tied" to some definite point of the displacement profile, but is "displaced" in the modulation direction when the crystal is rotated. From the condition $\cos \varphi_3 < 1$ we can determine the range of θ in which third solutions can exist.

Relations (8) and (9) permit the spectral peaks to be tied in with points on the displacement profile.

III. EXPERIMENTAL RESULTS AND DISCUSSION

In Sec. II we obtained a quantitative relation between the orientation dependence of the positions of the peaks of the anomalous spectral distribution, on the one hand, and the EFG tensor components in a modulated structure, on the other. The EFG tensor is determined by following the following most efficient measurement procedure:

1. Determine the EFG tensor at a given structure in the basic structure from measurements of the second-order quadrupole shift of the central component of the spectrum, using the method of Ref. 13.

2. Plot the orientation dependences of the line shape at a certain fixed temperature in the incommensurate phase as the crystal is rotated in a magnetic field about the three mutually perpendicular axes of the laboratory frame. After plotting the orientational dependences of the frequencies of the terminal maxima of the spectral distribution, determine the quantities $\alpha_{ij}(T_1 - T_i)^\beta$ and $\alpha_{ii}(T_1 - T_i)^{2\beta}$ from relations (8). These quantities are indicative of the modulation corrections at the maximum positive and negative displacement points in the modulation wave. They vary sinusoidally along the displacement profile and can thus be easily determined at any point z_i .

3. Obtain, at a fixed crystal orientation in the magnetic field, the temperature dependences of the line shape in the entire region of existence of the incommensurate phase, and determine from them the exponent β . Since α_{ij} and α_{ii} are constants, this will also determine the EFG tensor at any temperature in the region where the plane-wave-modulation approximation is applicable. It was established in Refs. 1, 2, 6, and 7 that in Rb_2ZnCl_4 and Rb_2ZnBr_4 this approximation describes well enough the entire incommensurate-phase region, except the immediate vicinity of T_c .

The EFG tensor in an incommensurate structure can undoubtedly be determined also when the basic-structure EFG tensor cannot be determined for some reason. In that case, to obtain information equivalent to that indicated above, one must plot the experimental orientation dependences of the line shape for three orthogonal rotations at several fixed temperatures. Such an experiment is very cumbersome, since the shape of the spectral distribution in the

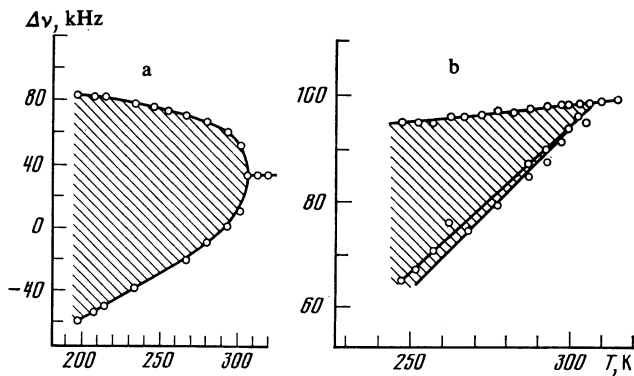


FIG. 1. Temperature dependences of the frequencies of the terminal peaks of the anomalous line shape of $^{87}\text{Rb}(1)$ in Rb_2ZnCl_4 : a—for crystal orientation $c \perp H_0$ in the magnetic field, with the angle $\theta = 25^\circ$ measured from the a axis; b—at crystal orientation $a \perp H_0$, $\theta = 3^\circ$ from the b axis.

incommensurate phase can usually be reliably recorded after prolonged accumulation of the signal.

We note that if weak spectrum satellites can be recorded, the use of relations (5) and (7) for the description of the first-order quadrupole effects permits also the EFG tensor to be determined in a modulated structure.

The NMR spectra of ^{87}Rb in Rb_2ZnCl_4 and Rb_2ZnBr_4 were recorded with a Brooker spectrometer in single-pulse sequence mode followed by Fourier transformation of the free-induction falloff at $\nu_L = 23.5$ MHz.

For crystal rotation about the axes b and c , Eq. (8) predicts a predominant contribution of the $\Delta\nu$ corrections lin-

ear in U_0 , and quadratic corrections to $\Delta\nu$ should predominate for rotation about the a axis. The temperature dependences of the frequencies of the terminal peaks for the $(\frac{1}{2} \rightarrow -\frac{1}{2})$ transition of ^{87}Rb were obtained at the corresponding crystal orientations in the magnetic field (Fig. 1). For the first case (Fig. 2a) the positions of the terminal peaks should be defined as $\nu_{\pm} = \nu_0 \pm A + B$, where $A \sim (T - T_I)^\beta$; for the second case $\nu_{\pm} = \nu_0 + B$, where $B \sim (T - T_I)^{2\beta}$. It can be seen from the figures that the experimental data correspond to the experimental geometry predicted by relations (8).

The parameter β determined from the temperature dependences (Fig. 1) changes from 0.36 to 0.34 with decreasing temperature everywhere in the incommensurate phase, except in the immediate vicinity of the phase-transition temperature T_I .

In the initial phase, the orientation dependences of the shift of the central component of the spectrum were obtained by rotating the crystals in a magnetic field about mutually perpendicular axes x , y , and z parallel to the axes of the rhombic cell of the paraelectric phase.

The data for $T > T_I$ are shown in Figs. 2a, 3a, 4a, and 5a. The data were reduced by the method of Ref. 13, and the EFG tensors at the ^{87}Rb nuclei in the paraelectric phases of Rb_2ZnCl_4 and Rb_2ZnBr_4 are listed in Tables I–IV. The data for Rb_2ZnCl_4 agree well with experimental curves obtained earlier near T_I with another sample.¹²

According to the structure data¹⁹ on Rb_2ZnBr_4 one of the principal axes of the EFG tensors in this crystal and in

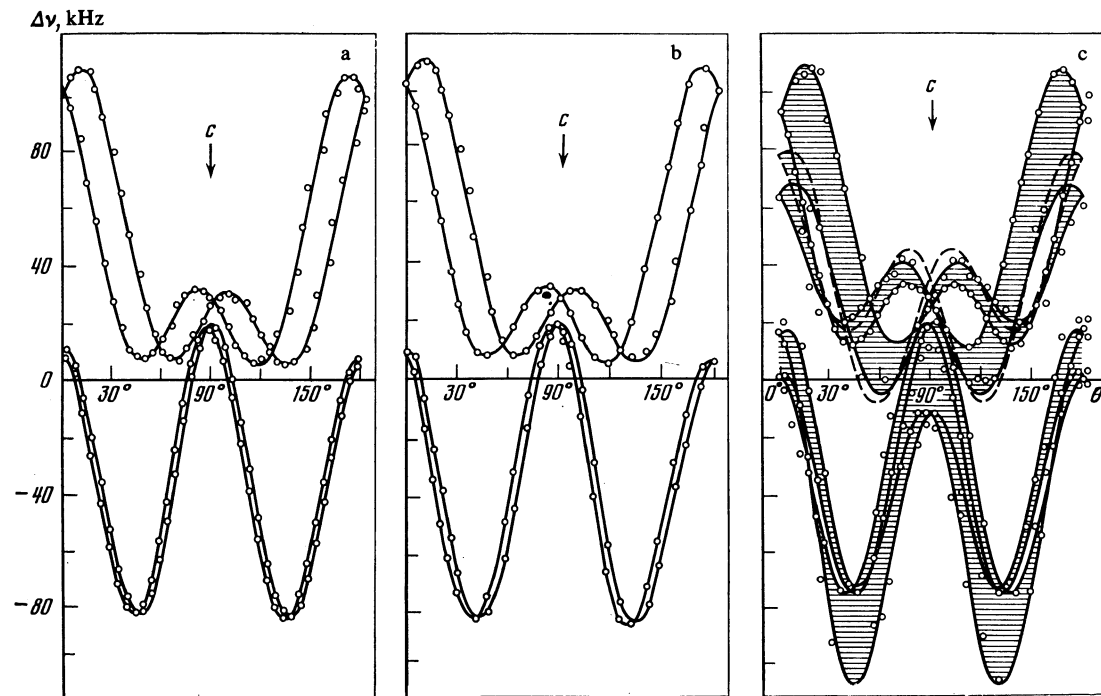


FIG. 2. Orientation dependences of the frequencies: a—of singlet lines $(\frac{1}{2} \rightarrow -\frac{1}{2})$ in the paraelectric phase of Rb_2ZnCl_4 ($T = 307 \text{ K} > T_I$); b—in the incommensurate phase in the immediate vicinity of $T_I = 289 \text{ K}$; c—of the edge peaks of the spectral distribution in the central region of the incommensurate phase ($T = 243 \text{ K}$). The crystal is rotated in the magnetic field about the a axis. Points—experimental values of the second-order shift $\Delta\nu$ of the central line relative to the Larmor frequency, solid lines; (a)—calculation by the method of Ref. 13, (b) and (c)—calculation from relation (8). The shaded areas show the continuum of the frequencies between the terminal peaks of the anomalous line of the modulated structure.

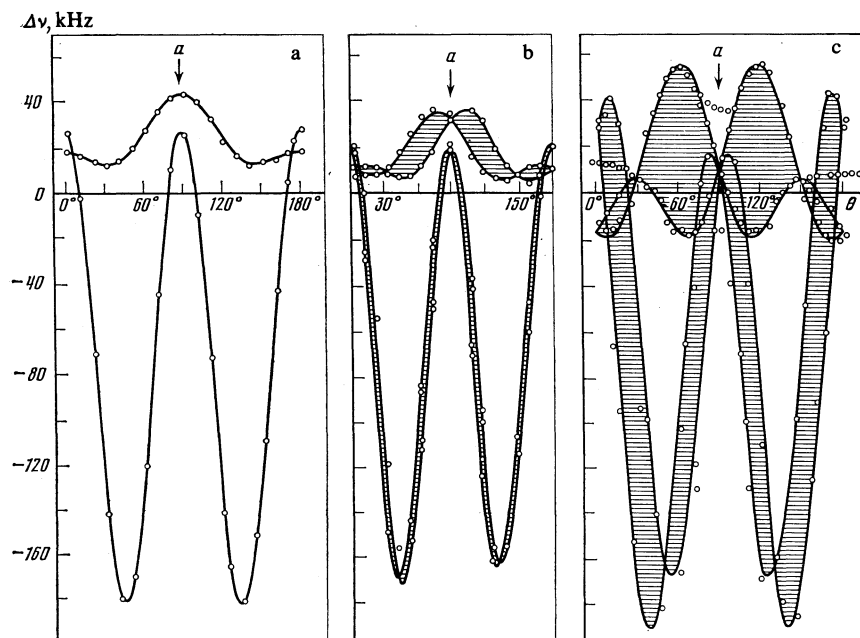


FIG. 3. Orientational dependences of the NMR frequencies ^{87}Rb in Rb_2ZnCl_4 as the crystal is rotated about the b axis. The notation and the temperature measurements are the same as for Fig. 2.

the isomorphous Rb_2ZnCl_4 is directed along the a axis for both lattice sites $\text{Rb}(1)$ and $\text{Rb}(2)$. The two other axes are rotated through a certain angle (see the Tables) in the \bar{m} symmetry plane, where all the Rb ions are localized. The effects observed below T_I are of the same type in both investigated crystals. Only the numerical values of the EFG parameters, listed in Tables I–IV, differ somewhat.

It was noted above (see Item 2 of the present section) that if the tensor V_{ij}^0 and the exponent β are established, the modulation corrections can be determined by merely mea-

suring the orientation dependences of the spectra at one fixed temperature in the incommensurate phase. We have nevertheless performed the corresponding measurements both in the immediate vicinity of T_I and in the middle region of the incommensurate phase, to check whether relations (5)–(8) hold.

The experimental data near T_I in the incommensurate phase are well described by relations (8) if we discard in them all the terms proportional to U_0^2 . The curves in Figs. 2b, 3b, 4b, and 5b correspond to this approximation. If the crystal is

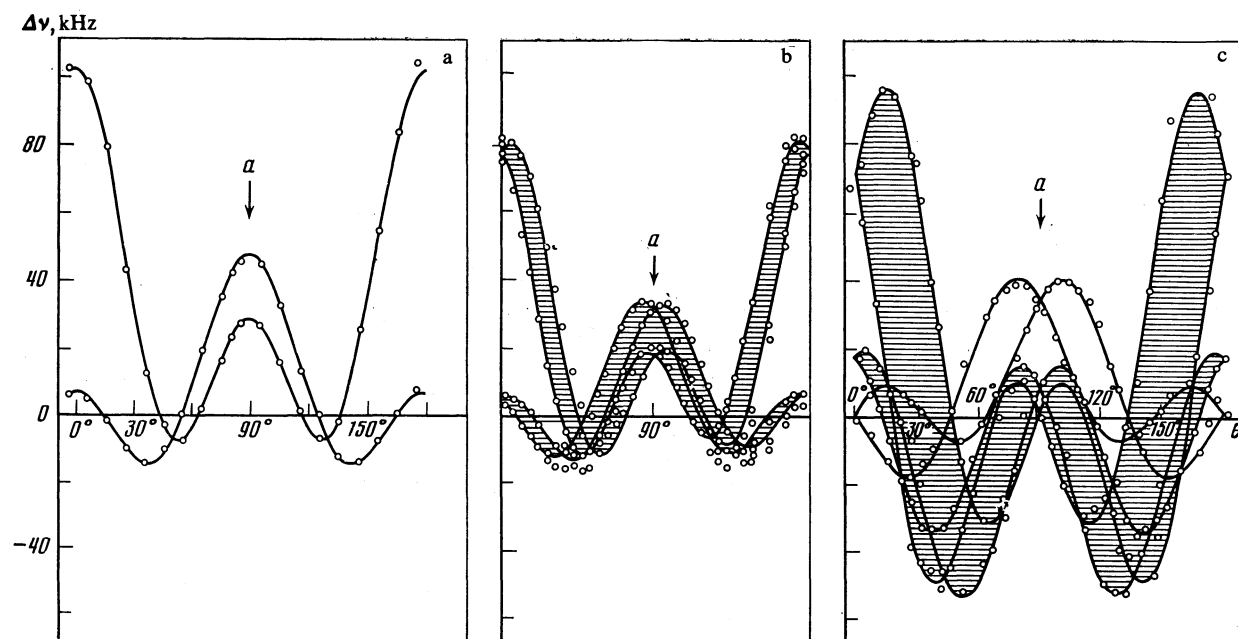


FIG. 4. Orientation dependences of the NMR frequencies of ^{87}Rb in Rb_2ZnCl_4 as the crystal is rotated about the b axis. The notation and temperatures are the same as in Fig. 2.

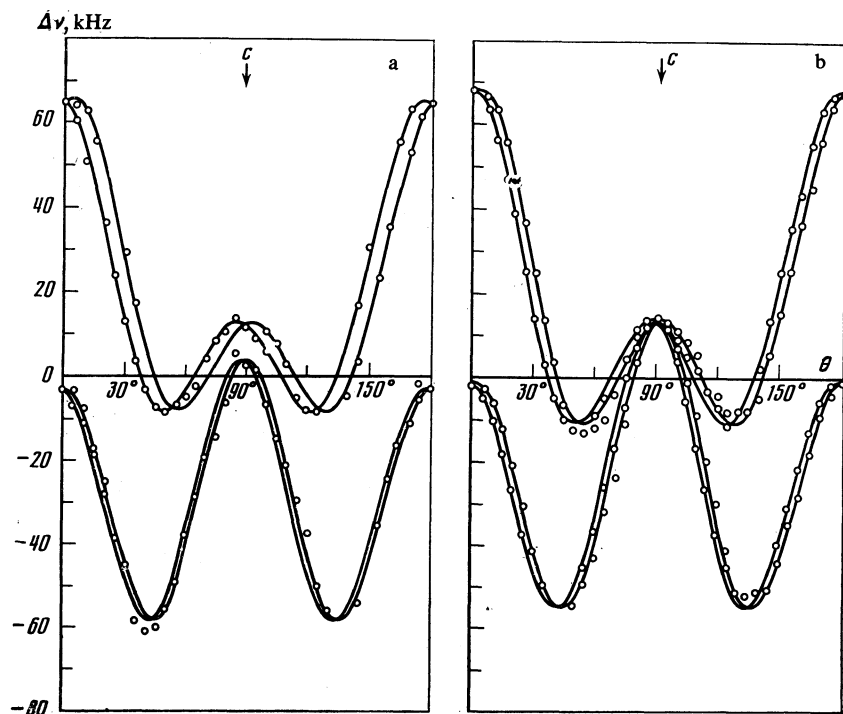


FIG. 5. Orientation dependences of NMR of ^{87}Rb in Rb_2ZnBr_4 for rotation about the c axis: a—paraelectric phase ($T = 370$ K); b—splitting of the frequency-continuum peaks in the incommensurate phase ($T = 333$ K). The notation is the same as in Fig. 2. The orientation dependences of the NMR frequencies as the Rb_2ZnBr_4 crystal is rotated about the a and b axes are given in Ref. 18.

rotated about the axis along which the displacements take place in the soft mode, there are no modulation effects and the curve observed is almost identical with the one for the initial phase (Figs. 2b and 5b). Rotation of the crystal about the two other axes introduces in (8) modulation corrections linear in U_0 . Figures 3b, c and 4b, c show the appearance of continuous distributions and agreement between the calculated curves and experiment. The values of $\alpha_{12} U_0$ and $\alpha_{13} U_0$ are determined from (8).

With decrease in temperature, the modulation corrections increase in accord with the temperature dependence of the order parameter, as is clearly seen from Figs. 2c, 3c, and 4c. If it is assumed that the splitting of the continuum peaks in Fig. 2c is due only to combinations, quadratic in U_0 , of the corrections α_{ij} to the off-diagonal components V_{ij}^0 , the edge-peak splittings shown dashed will be obtained. Agreement between the calculation and the experimental data (solid curves) at 243 K was obtained for all three rotations by including in (8) corrections of the type $\alpha_{ii} U_0^2$ to the diagonal

tensor components V_{ii}^0 . In Tables I–IV are given the EFG tensors at the points of the maximum positive and negative lattice displacements of the ^{87}Rb in the modulation waves. As expected, the components V_{xy} and V_{xz} , which are connected with the modulation corrections, increase with decreasing temperature, while the component V_{yz} varies within the limits of the usual “noncritical” temperature dependence.

The modulation effect consists mainly of rotation of the principal axes of the EFG tensors about the cell axes (see Tables II and IV). The angles that indicate the directions of the principal axes of the EFG tensors in the amplitudes of the displacement profile can be easily determined from the data of Tables II and IV. Along the displacement profiles there exists a continuous distribution of the rotation angles (of the “color” corrections), of cosinusoidal form, between the positive and negative maximum amplitudes, with passage through the orientation typical of the initial basic lattice.

TABLE I. EFG tensors (in MHz) at the ^{87}Br nuclei in Rb_2ZnBr_4 in a fixed coordinate system (a , b , c) in the paraelectric and incommensurate phases, determined from the orientation dependences of the NMR frequencies. The tensors determined in the incommensurate phase correspond to the positions of the maximum values of the positive and negative displacements in the modulation wave.

Temperature	Rb(1)			Rb(2)		
$T=370\text{K} > T_I$	4.28	0.00	0.00	0.78	0.00	0.00
		0.31	± 0.17		-3.11	± 0.12
			-4.59			2.33
$T=333\text{K} < T_I$	4.60	± 0.49	± 0.32	0.76	± 0.48	± 1.09
		0.01	± 0.29		-3.10	± 0.09
			-4.60			2.35

TABLE II. Principal values of γ_i (in MHz) and direction cosines μ_i of the quadrupole interaction tensors (eQV_{ii}/η) of ^{87}Rb in Rb_2ZnBr_4 relative to the rhombic cell axes $a < c < b$ in the paraelectric and incommensurate phases. The tensors in the incommensurate phase correspond to the positions of the maximum positive and negative displacements in the modulation wave.

Nucl.	Parameter	$T = 370 \text{ K} > T_I$			$T = 333 \text{ K} < T_I$			
		γ_i	μ_a	μ_b	μ_c	γ_i	μ_a	μ_b
Rb(1)	γ_i	4.28	0.32	-4.60	4.66	-0.33	-4.63	
	μ_a	1.0000	0.0000	0.0000	0.9935	± 0.1089	± 0.0315	
	μ_b	0.0000	0.9994	± 0.0346	± 0.1069	0.9925	± 0.0591	
	μ_c	0.0000	± 0.0346	0.9994	± 0.0376	± 0.0553	0.9978	
Rb(2)	γ_i	2.33	0.78	-3.11	2.921	0.250	-3.16	
	μ_a	0.0000	1.0000	0.0000	± 0.4589	0.8798	± 0.1238	
	μ_b	± 0.0220	0.0000	0.9998	± 0.0498	± 0.1136	0.9923	
	μ_c	0.9998	0.0000	± 0.0220	0.8870	± 0.4615	± 0.0083	

Figure 3b shows near the values 0, 90, and 180° sets of points with weak orientation dependences of the frequency. The points do not fit the calculated curves corresponding to the positions of the terminal peaks of the frequency continuum. The spectrum extrema, which exist in limited range of angles θ , correspond to satisfaction of the inequality $\cos \varphi_3 < 1$ and are described by relation (9) ("third solutions") in the approximation of the frequency by terms linear and quadratic in U_0 .

When the Rb_2ZnCl_4 axis was rotated around the c axis, additional spectral peaks (marked by the filled circles in Fig. 4c) were recorded in the incommensurate-phase region ($T = 243 \text{ K}$). These peaks have an orientation dependence of the same type as the terminal extrema observed at all θ , but do not correspond to the maximum amplitudes of the incommensurate displacements, nor are they described by Eq. (8).

It is most probable that their appearance is due to the onset of intensity centers at the impurities, i.e., to order-parameter phase pinning by crystal imperfections. This question is of interest not only from the point of view of complete interpretation of the NMR spectrum of the incommensurate structure. The behavior of certain macroscopic characteristics, such as the anomalous temperature hysteresis of the dielectric constant in incommensurate structures,¹⁸ is treated from the viewpoint of different effects of the pinning of the phase of the order parameter by impurities. The

possibility of observing these effects by microwave-spectroscopy methods uncover interesting prospects.

In the description of the symmetry properties of the modulation cell it was clearly shown how a symmetry element of the basic structure (the m plane) is conserved in the modulated phase at the color-symmetry level. The experimental orientation dependences (Figs. 3b,c and 4b,c) illustrate this fact, and Figs. 2b,c demonstrate the preservation, in the incommensurate phase, of planes perpendicular to the plane m , namely the curves symmetric about the b and c axes in Figs. 2a and 5a pertain to Rb nuclei bound in the unit cell of the initial phase by reflection planes perpendicular to m . Below T_I one can see four spectral continua (Figs. 2b,c and Rb) that are pairwise connected by the same symmetry element, but exist now only at the generalized-symmetry level.

Microwave-spectroscopy data demonstrate thus the law of conservation of the abstract symmetry in incommensurate-commensurate phase transitions. For crystals of the K_2SeO_4 family this law can be represented by the following scheme:

$$\Phi^{(\omega)} = P_{c^{(s)}+d^{(\omega)}} \frac{2_1^{(2)}}{c} \frac{2_1}{m^{(2)}} \frac{2_1^{(2)}}{n} \leftrightarrow p \frac{2_1}{c} \frac{2_1}{m} \frac{2_1}{n} = \Phi.$$

The description of incommensurate structures in terms of position color symmetry is certainly not an alternative to description by n -dimensional space groups. The mutual rela-

TABLE III. EFG tensors (in MHz) at the ^{87}Rb nuclei in Rb_2ZnCl_4 in a fixed coordinate frame (a , b , c) in the paraelectric and incommensurate phases, determined from the orientation dependences of the NMR frequencies. The tensors in the incommensurate phase correspond to the positions of the maximum positive and negative displacements in the modulation wave.

Temperature	Rb(1)			Rb(2)		
$T=307 \text{ K} > T_I$	-5.46	0.00	0.00	0.52	0.00	0.00
		0.26	± 0.82		-3.78	± 0.15
			5.20			3.26
$T=299 \text{ K} < T_I$	-5.48	0.65	± 0.30	0.48	± 0.40	± 0.70
		0.24	± 0.80		-3.75	± 0.20
			5.24			3.27
$T=243 \text{ K} < T_I$	-5.17	± 1.81	± 0.98	0.55	± 0.83	± 2.07
		0.40	± 0.93		-3.69	± 0.08
			4.78			3.13

TABLE IV. Principal values of γ_i (in MHz) and direction cosines of the quadrupole interaction tensor (eQV_{ii}/η) of ^{87}Rb in Rb_2ZnCl_4 relative to the paraelectric-phase axes a , b , and c . The tensors in the incommensurate phase correspond to the positions of positive and negative displacements in the modulation field. Since the experimental results of the preceding work¹² and the present one practically coincide in the close vicinity of T_I , the EFG tensors were not recalculated.

Nucleus	Parameter	$T = 307 \text{ K} > T_I$			$T = 299 \text{ K} < T_I$ [12]			$T = 243 \text{ K} < T_I$		
		γ_1	γ_2	γ_3	γ_1	γ_2	γ_3	γ_1	γ_2	γ_3
Rb (1)	γ_i	$\gamma_1=5.33$	$\gamma_2=0.13$	$\gamma_3=-5.46$	$\gamma_1=5.37$	$\gamma_2=0.20$	$\gamma_3=-5.57$	$\gamma_1=5.15$	$\gamma_2=0.61$	$\gamma_3=-5.75$
	μ_a	0.0000	0.0000	1.0000	± 0.0182	± 0.1202	0.9926	± 0.1333	± 0.2466	0.9599
	μ_b	± 0.1596	0.9872	0.0000	± 0.1519	0.9816	± 0.1161	± 0.2393	0.9319	± 0.2726
	μ_c	0.9872	± 1596	0.0000	0.9882	± 0.1486	± 0.0362	0.9618	± 0.2660	± 0.0652
Rb (2)	γ_i	$\gamma_1=3.26$	$\gamma_2=0.52$	$\gamma_3=-3.78$	$\gamma_1=3.44$	$\gamma_2=0.36$	$\gamma_3=-3.80$	$\gamma_1=4.29$	$\gamma_2=-0.42$	$\gamma_3=-3.88$
	μ_a	0.0000	1.0000	0.0000	± 0.2285	0.9685	± 0.0992	± 0.4904	0.8440	± 0.2171
	μ_b	± 0.0213	0.0000	0.9998	± 0.0144	± 0.1052	0.9943	± 0.0420	± 0.2260	0.9732
	μ_c	0.9998	0.0000	± 0.0213	0.9734	± 0.02258	± 0.0193	0.8705	± 0.4864	± 0.0754

tion between these approaches is known (see, e.g., Ref. 20).

The use of color position symmetry is convenient for the description of the local properties of incommensurate phases and, naturally, for microwave spectroscopy. On the other hand, to describe x-ray diffraction or the selection rules in optical spectra it is apparently more convenient to use four-dimensional space groups.¹⁵

In methods where the crystal is regarded as a continuous medium, it suffices to use conservation of point symmetry in commensurate-incommensurate phase transitions,²¹ which certainly does not contradict the resonance experiment.

The $\Delta\nu(T)$ temperature dependence (Fig. 1a) was obtained by one of us in the laboratory of Professor R. Blinc in Ljubljana. The authors are grateful for the opportunity to perform the measurements and for help. The authors thank L. I. Faleev and A. A. Sukhovskii for help with the calculations.

¹A. K. Moskalev, I. A. Belobrova and I. P. Aleksandrova, *Fiz. Tverd. Tela (Leningrad)* **20**, 3288 (1978) [*Sov. Phys. Solid State* **20**, 1896 (1978)].

²A. K. Moskalev, I. A. Belobrova, I. P. Aleksandrova, Sh. Sawada, and Y. Shiroishi, *Phys. St. Sol. (a)* **50**, K157 (1978).

³R. Osredkar, S. Juznic, V. Rutar, J. Seliger, and R. Blinc, *Ferroelectrics* **24**, 147 (1980).

⁴R. Blinc, V. Rutar, J. Seliger, S. Zumer, Th. Raising, and I. P. Aleksandrova, *Sol. St. Commun.* **34**, 895 (1980).

⁵R. Blinc, S. Juznic, V. Rutar, J. Seliger, and S. Zumer, *Phys. Rev. Lett.* **44**, 609 (1980).

⁶I. P. Aleksandrova, R. Blinc, B. Topic, S. Zumer, and A. Rigamonti, *Phys. St. Sol. (a)* **61**, 95 (1980).

⁷I. P. Aleksandrova, A. K. Moskalev and I. A. Belobrova, *J. Phys. Soc. Japan Suppl. B-86* (1980).

⁸B. H. Suits, S. Couturie, and C. P. Slichter, *Phys. Rev. Lett.* **45**, 194 (1980).

⁹R. Blinc, I. P. Aleksandrova, A. S. Chaves, F. Milia, V. Rutar, J. Seleger, B. Topic, and S. Zumer, *Sol. St. Phys.* **C15**, 547 (1982).

¹⁰A. S. Chaves, R. Gazzinelli, and R. Blinc, *Sol. St. Commun.* **37**, 123 (1981).

¹¹M. Fukui, S. Sumi, I. Hatta, and R. Abe, *Jpn. J. Appl. Phys.* **19**, 1559 (1980).

¹²V. Rutar, J. Seliger, B. Topic, R. Blinc, and I. P. Aleksandrova, *Phys. Rev.* **B24**, 2397 (1981).

¹³G. M. Volkoff, *Canad. J. Phys.* **31**, 820 (1953).

¹⁴P. M. De Wolf, *Acta Cryst.* **A33**, 493 (1977).

¹⁵A. Janner and T. Janssen, *Phys. Rev.* **B15**, 643 (1977).

¹⁶F. Borsa and A. Rigamonti, *J. Magn. Res.* **20**, 232 (1975).

¹⁷A. D. Bruce and R. A. Cowley, *J. Phys. C* **11**, 3609 (1978).

¹⁸I. P. Aleksandrova, S. Grande, Yu. N. Moskvich, A. I. Krieger, and B. A. Koptsik, *Phys. St. Sol. (b)* **115**, 603 (1983).

¹⁹K. Homano, Y. Ikeda, T. Fujimoto, K. Ema, and S. Hirotsu, *J. Phys. Soc. Jpn.* **49**, 2278 (1980).

²⁰V. A. Koptsik, *Zakony razvitiya slozhnykh sistem (Laws of Development of Complex Systems)*, L. Nauka, p. 152 (1980).

²¹V. A. Golovko and A. P. Levanyuk *Fiz. Tverd. Tela (Leningrad)* **23**, 3170 (1981) [*Sov. Phys. Solid State* **23**, 1850 (1981)].

Translated by J. G. Adashko